Space Weather Workshop
March 17-21, 2025
Boulder, CO

Drivers of Co-Occurring GICs During September 2017 Geomagnetic Storm

Bhagyashree Waghule[1], Delores J. Knipp[1]
[1]CU Boulder Smead Aerospace Engineering Sciences

OPEN TO WORK
LinkedIn

INTRODUCTION MOTIVATION AND BACKGROUND

Geomagnetically Induced Currents

- GICs are produced during Geomagnetic storms.
- Flow through long conducting cables such as power lines, pipelines.
- Large amplitude spikes can cause voltage destabilization in a power system.
- Sustained moderate amplitude GICs can cause overheating in the system. Pipelines may become susceptible to corrosion.

Sun-to-mud

- Eruption from Sun in form of Coronal Mass Ejection (CME) perturbs Earth's geomagnetic field (**B-field**).
- Currents flowing through the geospace (**J**) (Magnetosphere and Ionosphere) respond to the perturbation and further produce dB (Ampere's law).
- Change in B-field produces geoelectric field (**Eg**) per Faraday's law.

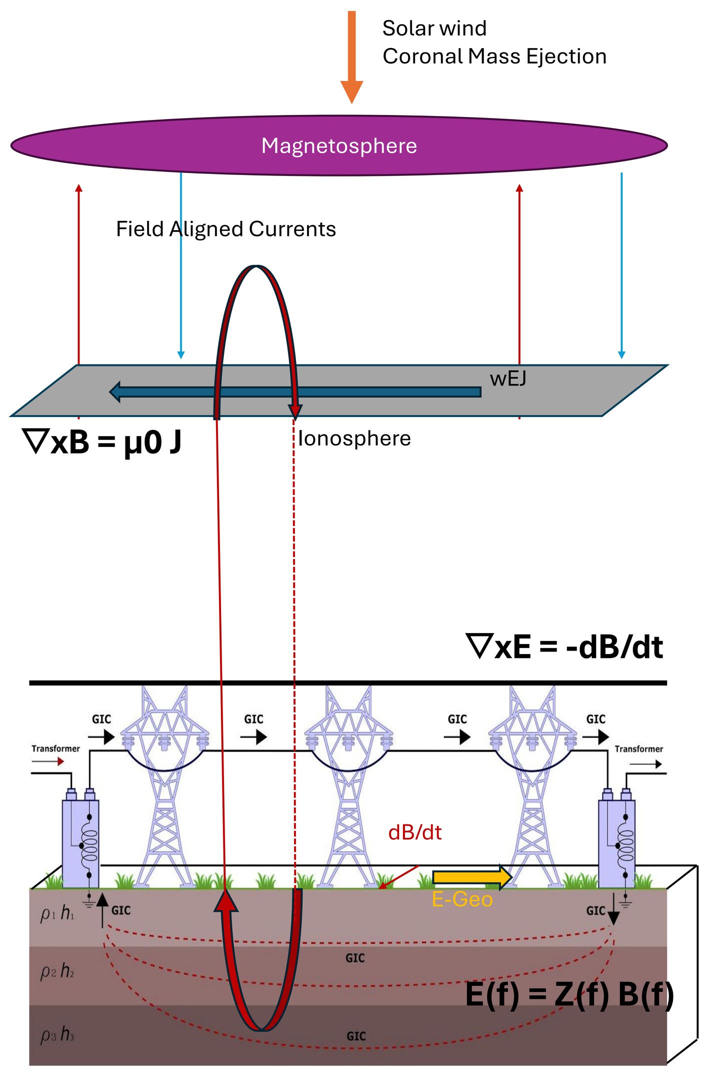

Figure 1: Illustration of how Sun-to-mud chain produces GICs. Underlying Equations shown

Key idea : GICs are a localized phenomena. Geoelectric field is a function of the interaction between B-field fluctuations and ground conductivity often formulated in frequency domain as E(f) = Z(f) B(f) where Z(f) is the 'skin depth'.

September 2017 Geomagnetic Storm

Long duration storm known for the 'double dip' in DST index.
Storm arrived early on 7th with northward IMF Bz and High density (not shown here) => Not Geoeffective

IMF Bz turns southward with pressure pulse at 23 UT on 7th => Geoeffective

IMF Bz turns northward from 02 – 11 UT on 8th -> First Recovery

IMF Bz turns southward 11:30 UT on 8th -> Magnetic Cloud arrival => Geoeffective

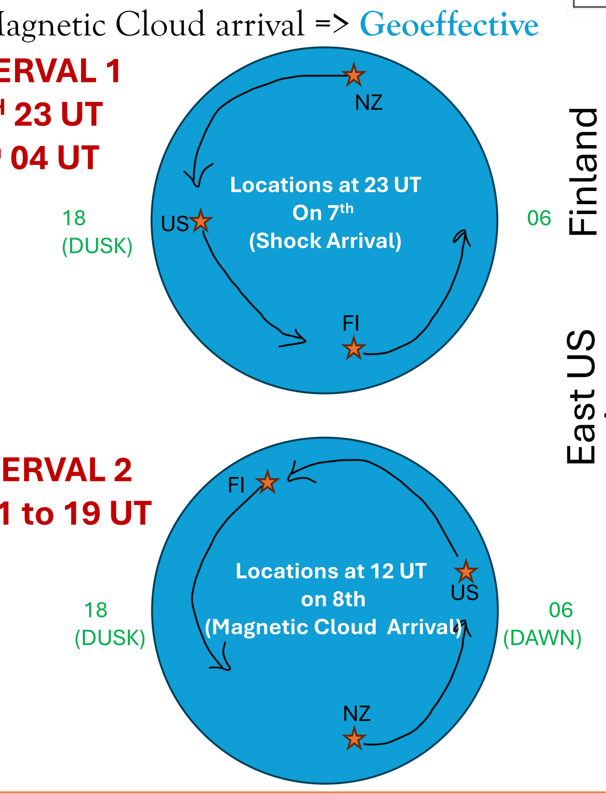

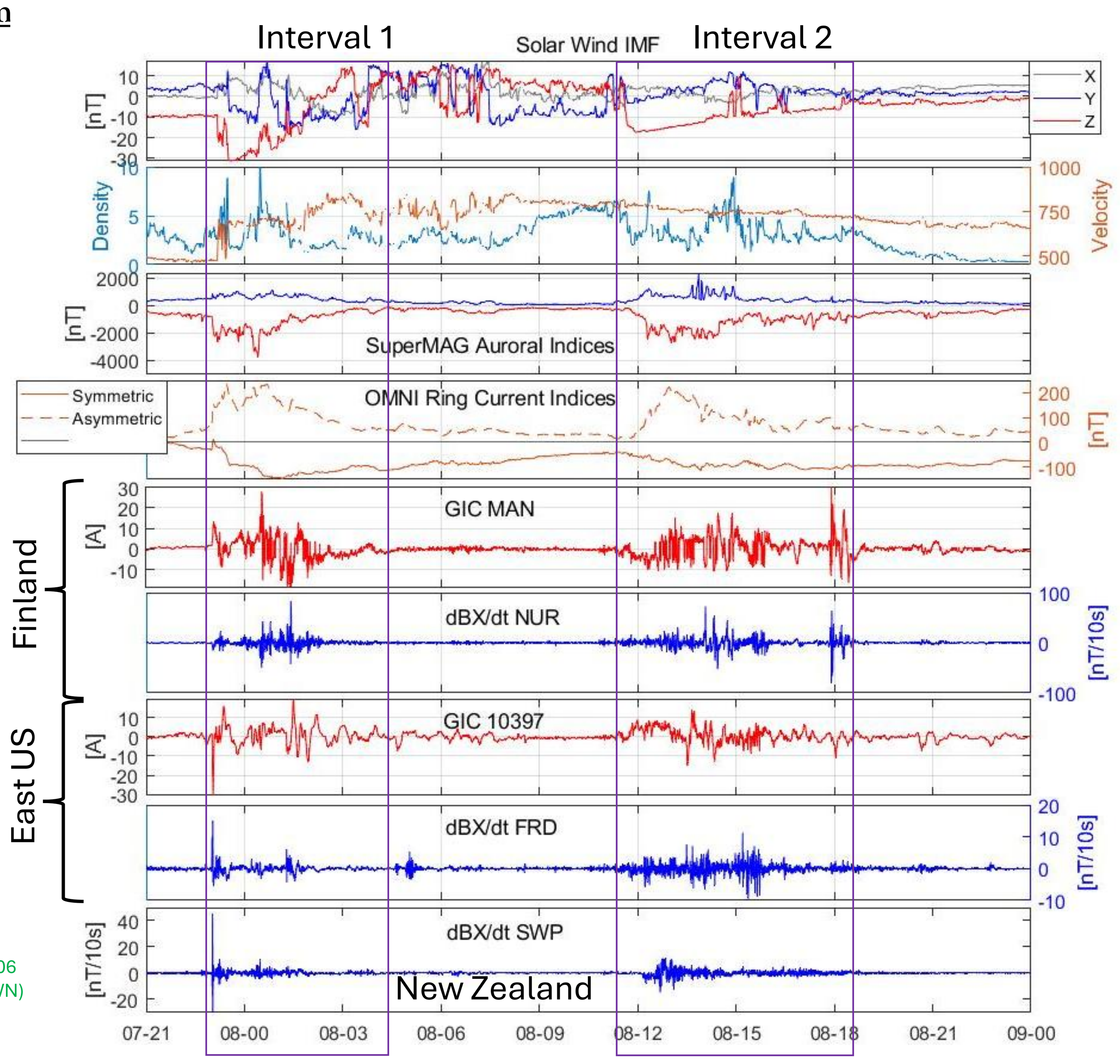

INTERVAL 1	INTERVAL 2
IMF Bz – rotates from south to north	IMF Bz – predominantly southward
Density pulses at 23 UT and 00:31 UT	Variable Density
Peak SML 00:30 UT	Peak SML 12-14 UT
Highly asymmetric RC First Main and Recovery Phase	Highly asymmetric RC Second Main and Recovery phase
Peak GIC (28A) at 00:31 UT Kola Peninsula Transformer[1] peak 85A at 22:20 UT	Peak GIC (30A) at 17:54 UT Kola Peninsula Transformer[1] peak 50A at 15:56 UT
Peak dBX/dt at 01:30 UT	Peak dBx/dt at 17:54 UT
Peak GIC (30A) at 23:03 UT (7th)	Peak GIC (15A) at 13:31 UT
Peak dBX/dt at 23:03 UT (7th)	Peak dBX/dt at 15:12 UT
Peak dBX/dt at 23:01 UT (7th) (Harmonic distortion at 01:30 UT[2])	Peak dBX/dt at 12:41 UT (Harmonic distortion at 12:45 UT[2])

[1]*Belakhovsky et al. 2019*
[2]*Clilverd et al. 2018*

Motivating Question: Although GICs are recorded globally, how do they differ with respect to local time? What localized Magnetosphere-Ionosphere activity drives these magnetic field fluctuations?

DATA AND METHOD

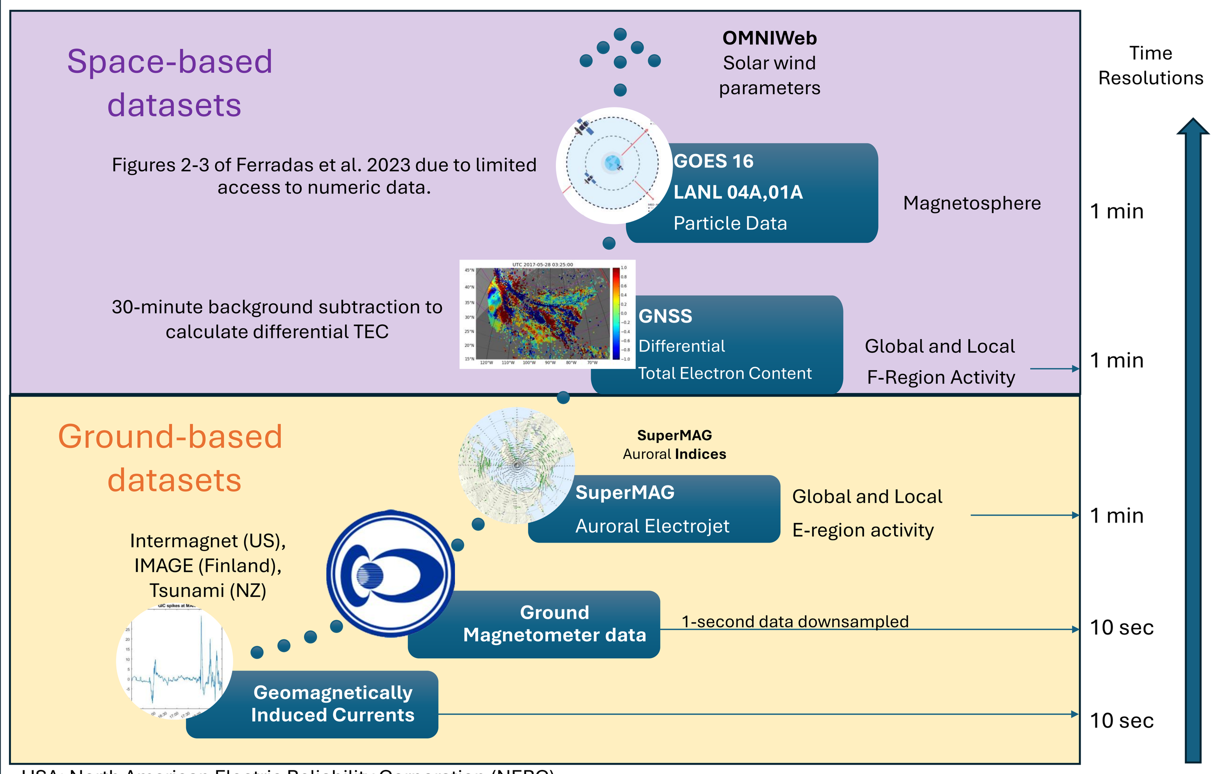

USA: North American Electric Reliability Corporation (NERC)
Finland: Mantsala Pipeline, Finnish Metereological Institute (FMI)
New Zealand: HalfwayBush T4 station (HWB) altered from Figure 5 of Clilverd 2019

Continuous Wavelet Transform (CWT) Analysis

Multiscale Decomposition of GIC and dBH timeseries

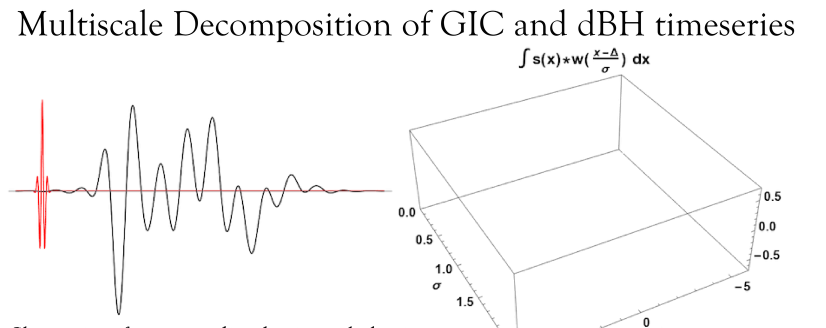

Shows time-frequency distribution – helps in understanding significant periodicities
Original work: Torrence & Compo (1999) + Grinsted et al. (2003)

Data Fusion

Observations from ground to space provide context for the multiscale time-frequency distribution shown in Continuous Wavelet Transform (Waghule et al. 2024)

RESULTS

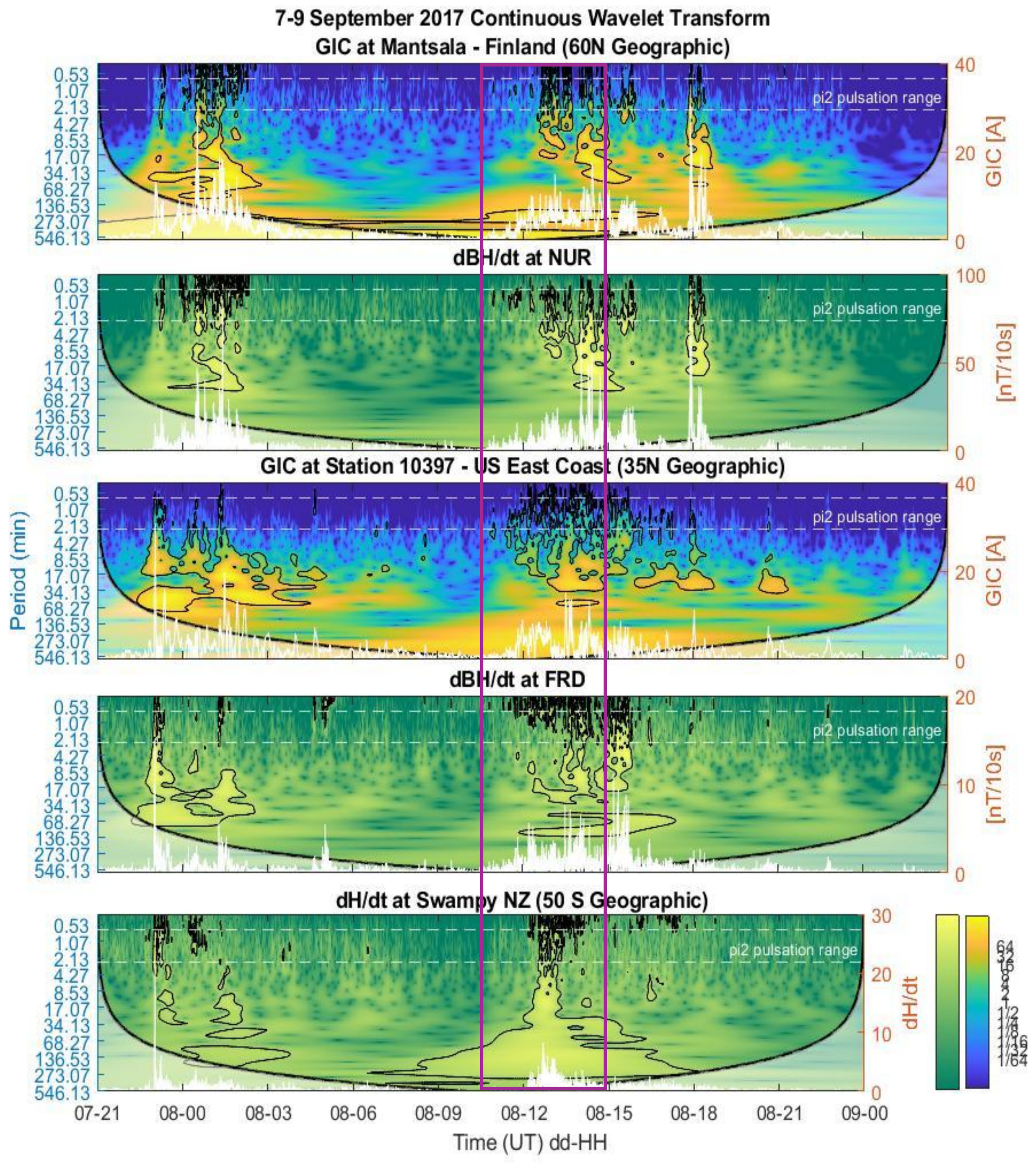

Figure: CWT of GIC shown in blue-yellow heatmap and CWT of dH/dt shown in green-yellow heatmap. Corresponding timeseries overlain on heatmap. Black contour lines shows area above background noise. 11-15 UT interval highlighted for Data Fusion shown to the right

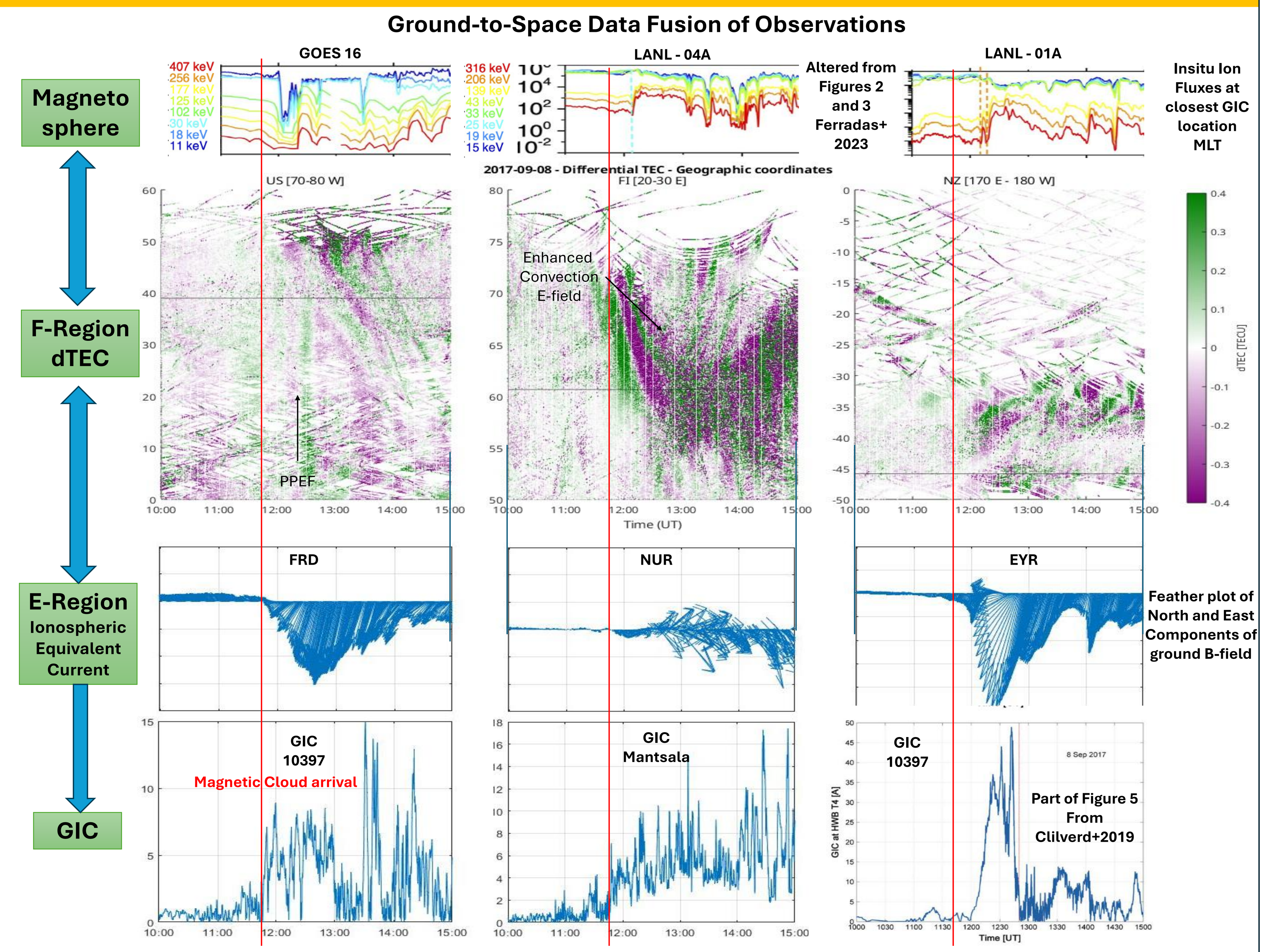

Figure: Data Fusion of Observations from Ground to Space. Red line marks the arrival time of Magnetic Cloud. Bottom to top: 1) GICs in Eastern US, Finland, and New Zealand. 2) Timeseries of Horizontal B-field component vectors (e.g. eastward overhead currents produce northward ground dB perturbation) 3) Keogram of dTEC. Green/Purple indicates TEC enhancement/depletion. 4) Insitu proton energy flux measurements at 6.6 Re (GEO). Satellites identified are closest to the MLT of interest.

RESULTS / DISCUSSION

- GICs were recorded globally during the G4 storm of September 2017
- Largest GICs in respective locations were recorded at different times
  - US – 23:03 UT on 7th; NZ – 12:45 UT on 8th; FI – 1754 UT on 8th
- More rapid fluctuations during the second interval (max SYMH < -146 nT) compared to the first interval (max SYM-H < -115 nT)

Continuous Wavelet Transform

- Multi-scale (multi-minute/broadband) disturbance in GIC and dBH corresponds to the two intervals at all three locations.
- High Frequency fluctuations especially in the Pi2 range indicate potential substorm injections (Saito 1969; Waghule 2024)
- More rapid fluctuations are recorded in the second interval compared to the first, indicating high global substorm activity.

10-15 UT Interval

- Key points from Data Fusion of observations:

Eastern US Dawn sector (5 to 10 MLT)

- **E-region:** Predominantly westward overhead ionospheric currents
- **F-region:** Sudden Global Disturbance (SGD, Zhang et al. 2023) at 12 UT
  - Prompt Penetration Electric Field (PPEF)
- **Magnetosphere:** small-scale Injections

Finland Afternoon Sector (12-17 MLT)

- **E-region:** rapidly fluctuation overhead ionospheric currents
  - Likely wave activity
- **F-region:** Expansion of auroral oval and intensification of convection E-field
- **Magnetosphere:** Injection at 12 UT followed by smaller injections from 13 UT.

New Zealand – Midnight Sector (22-03 MLT)

- **E-region:** Predominantly westward overhead ionospheric currents - abrupt change at 12:45 UT
- **F-region:** Large Travelling Ionospheric Disturbances (TIDs)
- **Magnetosphere:** Three distinct injection signals at 12, 14, 14:30 UT

CONCLUSION

How do co-occurring GICs vary with local time?

- Globally occurring GICs have different wave forms and peaks within the larger disturbance. Between 12-15 UT, GICs peak at night first, then dawn, and afternoon. Mid-latitude high frequency fluctuations indicates equatorward expansion of auroral oval.

What localized Magnetosphere-Ionosphere (M-I) activity drives these magnetic field fluctuations?

- The 10-15 UT interval GICs at all three locations were driven by substorm injections in the magnetosphere, but the E and F region data indicate different activity.
  - Eastern US sector shows substorm PPEF
  - This suggests that the coupled M-I system, which is a function of local time, controls the mesoscale ground B-field fluctuations.

Future work:
What drove the largest GIC spikes in Eastern US at 23 UT on 7th and in Mantsala at 17:54 UT?

ACKNOWLEDGEMENT AND REFERENCES

BW and DJK are funded by NSF Award 1933040 and NASA Award 80NSSC20K1784. We thank the data providers. IMAGE for NUR data, FMI for GIC data, SuperMAG for ground dB data, MIT Haystack team for differential TEC data. The authors thank C. J. Rodger, J. Malone-Leigh and the rest of the Otago University Space Physics group for the Solar Tsunamis MANA network data

Belakhovsky, V. B., Pilipenko, V. A., Sakharov, Ya. A., & Selivanov, V. N. (2019). SUBSTORM INFLUENCE ON GIC REGISTERED IN ELECTRIC POWER LINES: THE MAGNETIC STORM OF 7-8 SEPTEMBER 2017. https://doi.org/10.25702/KSC.2588-0039.2019.42.9-12

Clilverd, M. A., Rodger, C. J., Brundell, J. B., Dalzell, M., Martin, I., Mac Manus, D. H., et al. (2018). Long-lasting geomagnetically induced currents and harmonic distortion observed in New Zealand during the 7–8 September 2017 disturbed period. Space Weather, 16, 704–717. https://doi.org/10.1029/2018SW001822

Ferradas CP, Fok M-C, Maruyama N, Henderson MG, Califf S, Thaller SA and Kress BT (2023), The effects of particle injections on the ring current development during the 7-8 September 2017 geomagnetic storm. Front. Astron. Space Sci. 10:1278820. doi: 10.3389/fspas.2023.1278820

Grinsted, A., Moore, J. C., & Jevrejeva, S. (2004). Application of the cross wavelet transform and wavelet coherence to geophysical time series. Nonlinear Processes in Geophysics, 11(5/6), 561–566. https://doi.org/10.5194/npg-11-561-2004

Saito, T. (1969). Geomagnetic pulsations. Space Science Reviews, 10(3), 319–412. https://doi.org/10.1007/BF00203620

Torrence, C., & Compo, G. P. (1998). A practical guide to wavelet analysis. Bulletin of the American Meteorological Society, 79(1), 61–78. https://doi.org/10.1175/1520-0477(1998)079<0061:APGTWA>2.0.CO;2

Waghule, B., Knipp, D. J., Gannon, J. L., Billet, D., Vines, S. K., & Goldstein, J. (2024). What drove the GICs >10 A during the 17 March 2013 event at Mäntsälä? A novel framework for distinguishing the magnetospheric sources. Space Weather, 22, e2024SW003980. https://doi.org/10.1029/2024SW003980

Zhang, S.-R., Nishimura, Y., Vierinen, J., Lyons, L. R., Knipp, D. J., Gustavsson, B. J., et al. (2023). Simultaneous global ionospheric disturbances associated with penetration electric fields during intense and minor solar and geomagnetic disturbances. Geophysical Research Letters, 50, e2023GL104250. https://doi.org/10.1029/2023GL104250